

## Static and dynamic analysis of circular beams using explicit stiffness matrix

Mohammad Rezaiee-Pajand\* and Niloofar Rajabzadeh-Safaei<sup>a</sup>

*Department of Civil Engineering, Faculty of Engineering, Ferdowsi University of Mashhad, Iran*

*(Received November 29, 2015, Revised June 29, 2016, Accepted July 12, 2016)*

**Abstract.** Two new elements with six degrees of freedom are proposed by applying the equilibrium conditions and strain-displacement equations. The first element is formulated for the infinite ratio of beam radius to thickness. In the second one, theory of the thick beam is used. Advantage of these elements is that by utilizing only one element, the exact solution will be obtained. Due to incorporating equilibrium conditions in the presented formulations, both proposed elements gave the precise internal forces. By solving some numerical tests, the high performance of the recommended formulations and also, interaction effects of the bending and axial forces will be demonstrated. While the second element has less error than the first one in thick regimes, the first element can be used for all regimes due to simplicity and good convergence. Based on static responses, it can be deduced that the first element is efficient for all the range of structural characteristics. The free vibration analysis will be performed using the first element. The results of static and dynamic tests show no deficiency, such as, shear and membrane locking and excessive stiff structural behavior.

**Keywords:** free vibration analysis; closed-form stiffness matrix; curved beam; equilibrium conditions; strain-displacement relationships; thin beam; Finite Element Method (FEM); thick beam

---

### 1. Introduction

Curved beam elements are beneficial in loads transferring into axial, shear and bending forces, unlike straight ones. It was found that analyzing the slender curved beam by isoperimetric elements causes too high structural stiffness. This phenomenon is called shear locking effect. Up to now, most of the previous researchers have used three dependent displacement fields for the curved beam. The inherent coupling of these functions is the most significant cause of the tendency to exhibit membrane locking. It is worth emphasizing, this effect, which creates errors, is not presented in the straight beams. The common formulation, which is based on independent displacement fields of the same order, leads to locking errors. At first, some investigators suggested higher-order elements, with high degrees of freedom or too many nodes.

These techniques made the solution process hard and time consuming. Based on the constant normal strain and linear curvature, Sabir and Ashwell (1971) introduced a novel shape function

---

\*Corresponding author, Professor, E-mail: [rezaiee@um.ac.ir](mailto:rezaiee@um.ac.ir)

<sup>a</sup>Master of Science, E-mail: [niloofarsafaei@gmail.com](mailto:niloofarsafaei@gmail.com)

combined of the polynomial and trigonometric terms. Results of the Dawe's numerical tests (1974), for both shallow and deep curved beams, showed that the fifth-order polynomial model and also the strain-based one gave satisfactory outcomes. Meck (1980) indicated that the uncoupled tangential and radial displacements are the main source of errors, unlike explicit representation of the rigid body motions. Based on this finding, many studies have developed curved beams with coupled displacement functions. Ishaguddin *et al.* (2013) presented two locking-free curved beam finite element models using coupled polynomial interpolations to eliminate the flexure and torsion locking effects. In another study, the reduced integration scheme was used by Stolarski and Belytschko (1982) to remedy locking phenomenon. In 1989, Pendian *et al.* eliminated the obstacles arising from interpolation fields of the same order. Choi and Lim (1993) developed a constant-strain/constant-curvature element, and a constant-strain/linear-curvature element based on the assumed strain fields. Afterwards, they (Choi and Lim 1995) suggested two and three-nodded curved beams based on the constant and linear strain functions.

Lee and Sin (1994) and Yang and Sin (1995) offered curved beam elements with assumed strains, especially curvature. Third-order radial displacement was used by Raveendranath *et al.* (1999). These investigators (Raveendranath *et al.* 2001) employed quadratic polynomial interpolation for flexural rotation and constructed a nine D.O.F element. Another way to avoid the structural excessive stiffening is using the hybrid-mixed method (Kim and Park 2008, Benedetti and Tralli 1989, Kim and Kim 1998, Kim and Lee 2008, Kim *et al.* 2014). In 1998, Litewka and Rakowski applied the flexibility method to determine precise forces and in 2001, they used exact shape functions in derivation of the stiffness and mass matrix. By adding the nodal shear strain  $\gamma$ , as a new degree of freedom, Krishnan and Suresh (1998) developed a cubic linear element. Heppler (1992) derived a Timoshenko curved beam element with trigonometric basis functions to recover the rigid body motions. Fourier  $p$ -elements were proposed by Leung and Zhu (2004) to avoid the ill-conditioning problems associated with high-order polynomials. The exact dynamic stiffness matrix was presented by Eisenberger and Efraim (2001), and the natural frequencies were those that caused the matrix to become singular. For the derivation of the stiffness matrix, they applied unit displacement or rotation at each degree of freedom for the element. It is obvious this procedure is not a finite element method and leads to some complexities. Using this procedure with the name of "Direct method" Jafari and Mahjoob (2010) developed a three-dimensional beam element with non-uniform cross section.

Yang *et al.* (2008) solved the equations of motion utilizing the Galerkin finite element method to model the free in-plane vibrations of curved beams. Furthermore, Gimena *et al.* (2010) employed the finite transfer method to solve the system of linear ordinary differential equations and finding the forces, moments, rotations, and displacements at any point of the curved beam. The transfer matrix is a result of the integration of the mentioned differential equations. In the case of static analysis, Gonzaga *et al.* (2014) presented the stiffness matrix, which is determined from the transfer matrix expression, only by reordering operations. It should be noted, this procedure no longer needed the energy theorems. Zhu and Meguid (2008) suggested a novel three-nodded curved beam element to ensure that its displacement interpolation functions could explicitly satisfy the inextensible bending mode condition for the membrane locking-free instead of the rigid body modes.

So far, most of the researchers have neglected the membrane-bending interaction by the virtue of thin beam's assumptions. Merely a few studies, considered the effect of retaining these terms in the compliance material matrix (Kim and Park 2008, Benedetti and Tralli 1989, Kim and Kim 1998, Kim and Lee 2008). In all the mentioned investigations, only the shape function was solitary

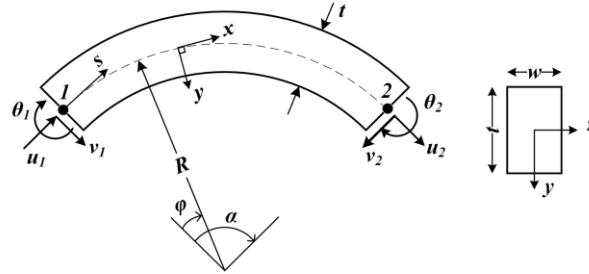


Fig. 1 General form of a curved beam

derived explicitly, and not the structural stiffness matrix. In this paper, a novel two-noded circular beam with six degrees of freedom will be proposed. Evidently, circular beams have constant curvature throughout their length. Therefore, these beams cannot be used when the arches have polynomial functions or any other shapes with variable curvatures. Anyway, for the case of circular beams by full integrating over the structural arch length, the relationship between forces and strains will be found. The approximate and exact forms of the obtained matrices will be demonstrated in section (4) and (5). Afterward, by satisfying equilibrium conditions, the accurate forces and strains will be achieved. Furthermore, based on the approximate compliance material matrix, the mass matrix will be obtained, and the closed-form beam stiffness matrix will be given in Appendix 1. Then, both proposed elements are compared in some static tests. Afterwards, the free vibration analysis will be performed by the first element. By utilizing the author’s scheme, a precise result with only one element per member can be found. Numerical findings confirm the merits of the presented formulations.

## 2. Strain-displacement equations

In this paper, two circular beams with two nodes and six degrees of freedom are modeled. A part of the element with central angle  $\alpha$ , constant thickness  $t$ , radius of curvature  $R$  and arch length  $l=R\alpha$  are illustrated in Fig. 1. By taking into account the shear effect, this beam is analyzed based on classical Timoshenko hypothesis (Reddy 1993). Each node has three displacements and three forces. The tangential displacement, radial displacement and rotation of the cross-section about the normal axis of the beam plane are represented by  $u$ ,  $v$  and  $\theta$ , respectively. Obviously, in-plane deformation causes axial, shear and bending stresses. Based on the displacement derivatives, the following equations indicate the strains vector,  $\{\varepsilon\}=\{\varepsilon_0 \ \gamma_0 \ \kappa\}$ , in the neutral axis.

$$\{\varepsilon\} = \begin{Bmatrix} \varepsilon_0 \\ \gamma_0 \\ \kappa \end{Bmatrix} = \begin{bmatrix} \frac{1}{R} \frac{d}{d\varphi} & -\frac{1}{R} & 0 \\ \frac{1}{R} & \frac{1}{R} \frac{d}{d\varphi} & -1 \\ 0 & 0 & \frac{1}{R} \frac{d}{d\varphi} \end{bmatrix} \begin{Bmatrix} u \\ v \\ \theta \end{Bmatrix}, \quad \varepsilon = \frac{1}{1-y/R}(\varepsilon_0 - y\kappa), \quad \gamma = \frac{\gamma_0}{1-y/R} \quad (1)$$

The relation between triple internal forces and strains on the beam reference surface can be obtained by integrating the stresses over the rectangular cross section. Accordingly, the next forces are available

$$\begin{aligned}
N_x &= \int_A \sigma \cdot dA = \int_{-t/2}^{t/2} E \cdot \frac{1}{1-y/R} (\varepsilon_0 - y\kappa) \cdot w \cdot dy \\
V_y &= \int_A \tau \cdot dA = \int_{-t/2}^{t/2} k \cdot G \cdot \frac{\gamma_0}{1-y/R} \cdot w \cdot dy \\
M_z &= -\int_A \sigma \cdot y \cdot dA = -\int_{-t/2}^{t/2} E \cdot \frac{y}{1-y/R} (\varepsilon_0 - y\kappa) \cdot w \cdot dy
\end{aligned} \tag{2}$$

The Young's modulus, shear modulus, area of the member's cross-section, bending moment of inertia about the neutral axis and the shear correction factor for this structure are  $E$ ,  $G$ ,  $A$ ,  $I$ ,  $k$ , respectively. Also, bending moment, axial and shear forces are presented by  $M_z$ ,  $N_x$  and  $V_y$ . In the general case, the exact compliance material matrix for the rectangular cross section has the below shape

$$[D_{m2}] = EA \begin{bmatrix} \frac{YR^2}{-1+YR^2} & 0 & \frac{R}{1-YR^2} \\ 0 & \frac{1}{X} & 0 \\ \frac{R}{1-YR^2} & 0 & \frac{R^2}{-1+YR^2} \end{bmatrix}, \begin{cases} X = \frac{tE}{kGR \cdot \ln\left(\frac{2R+t}{2R-t}\right)} \\ Y = \frac{\ln\left(\frac{2R+t}{2R-t}\right)}{R(R \cdot \ln\left(\frac{2R+t}{2R-t}\right) - t)} \end{cases} \tag{3}$$

By considering  $\varepsilon = D_m^{-1} \cdot \sigma$ , the subsequent strain fields can be achieved

$$\begin{Bmatrix} \varepsilon_0 \\ \gamma_0 \\ \kappa \end{Bmatrix} = \frac{1}{EA} \begin{bmatrix} 1 & 0 & \frac{1}{R} \\ 0 & X & 0 \\ \frac{1}{R} & 0 & Y \end{bmatrix} \begin{Bmatrix} N_x \\ V_y \\ M_z \end{Bmatrix} \tag{4}$$

In the case of considering slender effects, most of the studies applied the approximate compliance material matrix in their analysis. Eliminating membrane-bending interaction, the approximate compliance material matrix can be written in the following form

$$[D_{m1}] = \begin{bmatrix} EA & 0 & 0 \\ 0 & kGA & 0 \\ 0 & 0 & EI \end{bmatrix} \tag{5}$$

Both approximate compliance material matrix  $[D_{m1}]$  and also the exact one  $[D_{m2}]$  will be utilized by the authors. In sections (4) and (5), the formulation based on the approximate and exact compliance material matrices will be performed, respectively.

### 3. Equilibrium equations

In the elastic domain, based on the minimum potential energy, the governing equations can be established. The static part of the potential function,  $\Pi$ , has the below shape

$$\Pi = U - W_e, \quad U = \frac{1}{2} \int_0^L \int_A \sigma^T \cdot \varepsilon \cdot dA \cdot ds, \quad W_e = \int_S \mathbf{u}^T \cdot \mathbf{F} \cdot ds + \sum_{i=1,2} \mathbf{P}_i \cdot \mathbf{u}_i \quad (6)$$

Herein,  $U$  and  $W_e$  represent the elastic strain energy and the work done by external loads, respectively. Moreover, the strain vector of the neutral axis, displacement vector, distributed load vector and nodal load vector are indicated by  $\varepsilon$ ,  $u$ ,  $F$  and  $P_i$  respectively. Furthermore, subscript  $i$  indicates the number of nodes. By substituting these parameters in the previous equalities, the next result is obtained

$$\begin{aligned} \Pi = \int_S \left( \frac{1}{2} [N_x \cdot (u_{,s} - \frac{v}{R}) + V_y \cdot (\frac{u}{R} + v_{,s} - \theta) + M_z \cdot (\theta_{,s})] - u \cdot p_x - v \cdot q_y - \theta \cdot m_z \right) \cdot ds - \\ \sum_{i=1,2} (u_i \cdot p_{xi} + v_i \cdot q_{yi} + \theta_i \cdot m_{zi}) \end{aligned} \quad (7)$$

The variation of the potential function,  $\delta\Pi=0$ , will lead to the next three equations of equilibrium

$$\begin{aligned} N_{x,s} - \frac{V_y}{R} = 0 & \qquad \qquad \qquad N_x = -c_1 \cdot \cos\varphi + c_2 \cdot \sin\varphi \\ V_{y,s} + \frac{N_x}{R} = 0 & \qquad \longrightarrow \qquad V_y = c_1 \cdot \sin\varphi + c_2 \cdot \cos\varphi \\ M_{z,s} + V_y = 0 & \qquad \qquad \qquad M_z = c_1 \cdot R \cdot \cos\varphi - c_2 \cdot R \cdot \sin\varphi + c_3 \end{aligned} \quad (8)$$

In former equalities, the subscript “, s” refers to the differentiating with respect to the longitudinal axis  $s$ . Also,  $c_1$ ,  $c_2$  and  $c_3$  are the integration constants, which are defined as the nodal unknowns.

#### 4. Approximate formulation

According to section (2), the membrane-bending interaction disappeared by considering  $t/R \ll 1$ . In the following equations, the strain functions are generated with respect to the internal forces

$$\begin{aligned} \varepsilon_0 &= \frac{1}{EA} (-c_1 \cdot \cos\varphi + c_2 \cdot \sin\varphi) \\ \gamma_0 &= \frac{1}{kGA} (c_1 \cdot \sin\varphi + c_2 \cdot \cos\varphi) \\ \kappa &= \frac{1}{EI} (R(c_1 \cdot \cos\varphi - c_2 \cdot \sin\varphi) + c_3) \end{aligned} \quad (9)$$

Solving a set of equilibrium equations will lead to the coming displacement fields

$$\left\{ \begin{array}{l} \theta = \int R \cdot \kappa \cdot d\varphi \\ u + u_{,\varphi\varphi} = R(\gamma_0 + \theta + \varepsilon_{0,\varphi}) \\ v = u_{,\varphi} - R \cdot \varepsilon_0 \end{array} \right\} \left\{ \begin{array}{l} u = c_1 \cdot \frac{\lambda}{2} (-\varphi \cos\varphi) + c_2 \cdot \frac{\lambda}{2} (\varphi \sin\varphi) + c_3 \cdot \beta \cdot \varphi + d_1 \cdot R + \\ \quad d_2 \cdot \sin\varphi + d_3 \cdot \cos\varphi \\ v = c_1 \cdot \left( \frac{\lambda}{2} \varphi \sin\varphi - \left( \frac{\lambda}{2} - \mu \right) \cos\varphi \right) + c_2 \cdot \left( \frac{\lambda}{2} \varphi \cos\varphi + \left( \frac{\lambda}{2} - \mu \right) \sin\varphi \right) + c_3 \cdot \beta + \\ \quad d_2 \cdot \cos\varphi - d_3 \cdot \sin\varphi \\ \theta = c_1 \cdot \beta \sin\varphi + c_2 \cdot \beta \cos\varphi + c_3 \cdot \frac{\beta \varphi}{R} + d_1 \end{array} \right.$$

$$\lambda = R\left(\frac{1}{kGA} + \frac{R^2}{EI} + \frac{1}{EA}\right) \quad , \quad \beta = \frac{R^2}{EI} \quad , \quad \mu = \frac{R}{EA} \quad (10)$$

The vector of the nodal unknowns has the below shape

$$\hat{\mathbf{q}}^T = [c_1 \quad c_2 \quad c_3 \quad d_1 \quad d_2 \quad d_3] \quad (11)$$

Having the nodal unknown resultants, the succeeding matrix can be derived from the strain and displacement interpolation functions

$$\boldsymbol{\varepsilon} = [\mathbf{B}_q] \hat{\mathbf{q}} \quad , \quad \mathbf{u} = [\mathbf{N}_q] \hat{\mathbf{q}} \quad (12)$$

$$[\mathbf{B}_q] = \begin{bmatrix} -\frac{1}{EA} \cdot \cos \varphi & \frac{1}{EA} \cdot \sin \varphi & 0 & 0 & 0 & 0 \\ \frac{1}{kGA} \cdot \sin \varphi & \frac{1}{kGA} \cdot \cos \varphi & 0 & 0 & 0 & 0 \\ \frac{R}{EI} \cdot \cos \varphi & -\frac{R}{EI} \cdot \sin \varphi & \frac{1}{EI} & 0 & 0 & 0 \end{bmatrix} \quad (13)$$

$$[\mathbf{N}_q] = \begin{bmatrix} \frac{\lambda}{2}(-\varphi \cos \varphi) & \frac{\lambda}{2}(\varphi \sin \varphi) & \beta \cdot \varphi & R & \sin \varphi & \cos \varphi \\ \frac{\lambda}{2} \varphi \sin \varphi - \left(\frac{\lambda}{2} - \mu\right) \cos \varphi & \frac{\lambda}{2} \varphi \cos \varphi + \left(\frac{\lambda}{2} - \mu\right) \sin \varphi & \beta & 0 & \cos \varphi & -\sin \varphi \\ \beta \sin \varphi & \beta \cos \varphi & \frac{\beta \varphi}{R} & 1 & 0 & 0 \end{bmatrix} \quad (14)$$

## 5. Exact formulation

Using Eq. (4), the strains can be written in terms of the internal forces, as follows

$$\begin{cases} \varepsilon_0 = \frac{1}{EA} \left( N_x + \frac{M_z}{R} \right) \\ \gamma_0 = \frac{1}{EA} (X \cdot V_y) \\ \kappa = \frac{1}{EI} \left( \frac{N_x}{R} + Y \cdot M_z \right) \end{cases} \Rightarrow \begin{cases} \varepsilon_0 = \frac{1}{EA} \left( \frac{c_3}{R} \right) \\ \gamma_0 = \frac{1}{EA} X (c_1 \cdot \sin \varphi + c_2 \cdot \cos \varphi) \\ \kappa = \frac{1}{EA} \left( c_1 \left( \frac{YR^2 - 1}{R} \cos \varphi \right) + c_2 \left( \frac{1 - YR^2}{R} \sin \varphi \right) + Y \cdot c_3 \right) \end{cases} \quad (15)$$

By utilizing Eq. (10), the displacement field will have the coming appearance

$$\begin{aligned} u &= c_1 (\eta (-0.5 \varphi \cos \varphi)) + c_2 (\eta (0.5 \varphi \sin \varphi)) + c_3 (\zeta \cdot R \varphi) + d_1 (R) + d_2 (\sin \varphi) + d_3 (\cos \varphi) \\ v &= c_1 (\eta (-0.5 \cos \varphi + 0.5 \varphi \sin \varphi)) + c_2 (\eta (0.5 \sin \varphi + 0.5 \varphi \cos \varphi)) + c_3 (\zeta) + d_2 (\cos \varphi) + d_3 (-\sin \varphi) \\ \theta &= c_1 (\zeta \cdot \sin \varphi) + c_2 (\zeta \cdot \cos \varphi) + c_3 (\zeta \cdot \varphi) + d_1 \end{aligned}$$

$$\zeta = \frac{YR^2 - 1}{EA}, \quad \zeta = \frac{YR}{EA}, \quad \xi = \frac{X}{EA}, \quad \eta = R(\zeta + \xi) \quad (16)$$

Eventually,  $\mathbf{B}_q$  and  $\mathbf{N}_q$  are required for introducing the beam stiffness matrix. They are given in the below lines

$$\begin{aligned} [\mathbf{N}_q] &= \begin{bmatrix} \frac{\eta}{2}(-\varphi \cos \varphi) & \frac{\eta}{2}(\varphi \sin \varphi) & \zeta R \varphi & R & \sin \varphi & \cos \varphi \\ \frac{\eta}{2}(-\cos \varphi + \varphi \sin \varphi) & \frac{\eta}{2}(\sin \varphi + \varphi \cos \varphi) & \zeta & 0 & \cos \varphi & -\sin \varphi \\ \zeta \sin \varphi & \zeta \cos \varphi & \zeta \varphi & 1 & 0 & 0 \end{bmatrix} \\ [\mathbf{B}_q] &= \begin{bmatrix} 0 & 0 & \frac{1}{EA} & \frac{1}{R} & 0 & 0 & 0 \\ \zeta \sin \varphi & \zeta \cos \varphi & 0 & 0 & 0 & 0 & 0 \\ \zeta \frac{\cos \varphi}{R} & -\zeta \frac{\sin \varphi}{R} & \frac{\zeta}{R} & 0 & 0 & 0 & 0 \end{bmatrix} \end{aligned} \quad (17)$$

## 6. Finite element formulation

Based on the Eq. (12), the nodal displacement vector is derived by substituting nodal  $\varphi$  into matrix form of the displacement interpolation function. This leads to coming equality

$$\hat{\mathbf{D}} = [\mathbf{G}_q] \hat{\mathbf{q}} \longrightarrow \hat{\mathbf{q}} = [\mathbf{G}_q]^{-1} \hat{\mathbf{D}}, \quad \hat{\mathbf{D}}^T = [u_1 \quad v_1 \quad \theta_1 \quad u_2 \quad v_2 \quad \theta_2] \quad (18)$$

Rewriting the displacement and strain interpolation functions in terms of nodal displacement results in the below functions

$$\begin{aligned} \mathbf{u} &= [\mathbf{N}_q] \cdot ([\mathbf{G}_q]^{-1} \hat{\mathbf{D}}), \quad \hat{\mathbf{N}} = [\mathbf{N}_q] \cdot [\mathbf{G}_q]^{-1} \\ \boldsymbol{\varepsilon} &= [\mathbf{B}_q] \cdot ([\mathbf{G}_q]^{-1} \hat{\mathbf{D}}), \quad \hat{\mathbf{B}} = [\mathbf{B}_q] \cdot [\mathbf{G}_q]^{-1} \end{aligned} \quad (19)$$

Using the new form of strains and displacements, the kinetic energy, strain energy and the work done by external loads can be written as follows

$$\begin{aligned} T &= \frac{1}{2} \int_s \{ \dot{\mathbf{u}} \}^T \cdot [m] \cdot \{ \dot{\mathbf{u}} \} \cdot ds = \frac{1}{2} \left( \int_s \rho \cdot A \cdot (\dot{u})^2 \cdot ds + \int_s \rho \cdot A \cdot (\dot{v})^2 \cdot ds + \int_s \rho \cdot A \cdot (\dot{\theta})^2 \cdot ds \right) \\ U &= \frac{1}{2} \int_s \{ \boldsymbol{\varepsilon} \}^T \cdot [\mathbf{D}_m] \cdot \{ \boldsymbol{\varepsilon} \} \cdot ds \\ W_e &= \int_s \{ \mathbf{u} \}^T \cdot \{ \mathbf{F} \} \cdot ds + \sum_{i=1,2} \{ u_i \}^T \cdot \{ P_i \} \end{aligned} \quad (20)$$

Where

$$[m] = \rho \begin{bmatrix} A & 0 & 0 \\ 0 & A & 0 \\ 0 & 0 & I \end{bmatrix} \quad (21)$$

In these equalities,  $\rho$  is the mass density, and the over-dot functions denote the derivatives with respect to the time. By employing the shape functions of Eq. (19) and exact integrating over the arch length of the beam the related mass matrix, stiffness matrix and load vector are achieved.

$$\begin{aligned} [M] &= \int_S [N]^T \cdot [m] \cdot [N] \cdot ds \\ [S] &= \int_S [B]^T \cdot [D_m] \cdot [B] \cdot ds \\ \{P\} &= \int_S [N]^T \cdot \{F\} \cdot ds + \{P_i\}_{i=1,2} \end{aligned} \quad (22)$$

The general form of the structural stiffness entries,  $S_{ij}$  based on the approximate compliance material matrix,  $D_{m1}$ , will be given in Appendix 1.

## 7. Numerical studies

Throughout this study, for the static tests,  $k$  is assumed 5/6. Two four-sided finite elements are proposed in this paper. The first and second elements are based on the approximate and exact compliance material matrices, respectively. Moreover, answers of the Castigliano's energy theorem are denoted by subscript  $c$ , and the first element's result will compare with this technique. Furthermore, the subscript  $f$  refers to the answers of the fine-mesh finite element method by utilizing four-sided Q8 element. Similarly, the results of the second element will be compared with the finite element and Castigliano's theorem answers. It should be noted, the free vibration analysis are performed by using the first element.

### 7.1 A quadrant cantilever ring

The geometry of a quadrant cantilever beam with unit width and  $R=0.254$  m (10in) is shown in Fig. 2. The Young's modulus and Poisson's ratio are used as 72.4 GPa ( $10.5E+06$  lbf/in<sup>2</sup>) and 0.3125, respectively.

The beam is bearing a radial concentrated load at the free end. This structure will be analyzed with only one two-nodded element. The results of the first and second suggested elements for the displacements versus the slenderness ratio are illustrated in Figs. 3-4. It should be added, responses of the second element are normalized with both finite element method and Castigliano's theorem. The answers of Lee and Sin (1994) methods, by using one element based on the curvature function, and also the outcomes of Raveendranath *et al.* (1999), by employing two

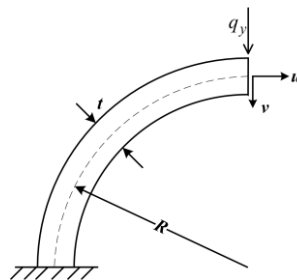


Fig. 2 The geometry of a quadrant cantilever ring

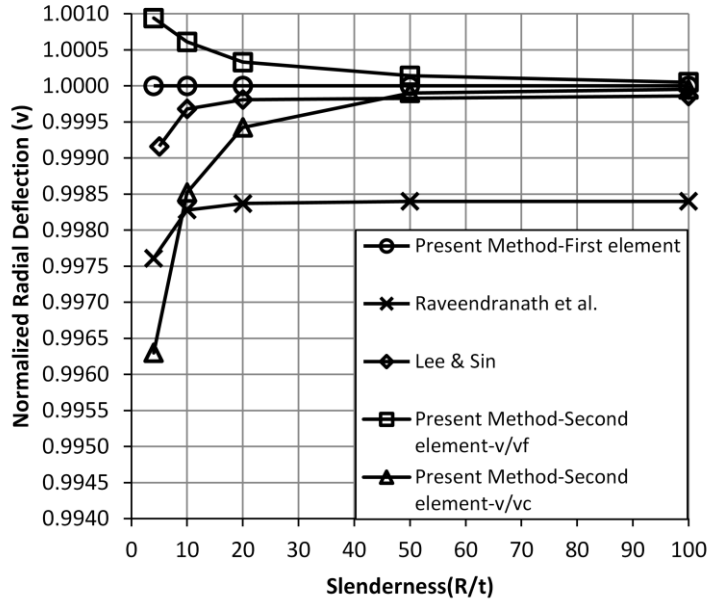


Fig. 3 The free end radial displacement for a quadrant cantilever ring under radial loading

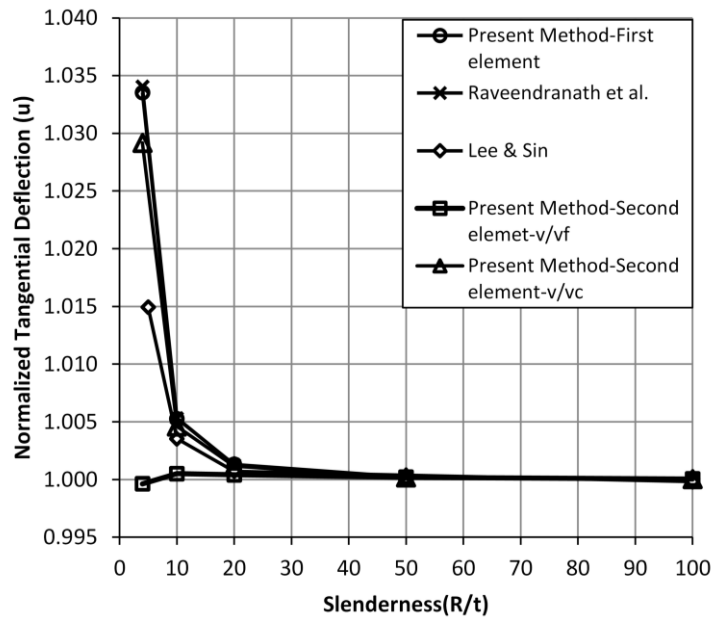


Fig. 4 The free end tangential displacement for a quadrant cantilever ring under radial loading

elements based on the third-order interpolation for radial displacement, will be utilized to demonstrate the suggested elements superiority. According to the Fig. 3,  $v/v_f$  of the second element has a negligible error in comparison with the other previously published values and also precise answer of the first element, while,  $v/v_c$  of the second element has more error. On the other hand, in

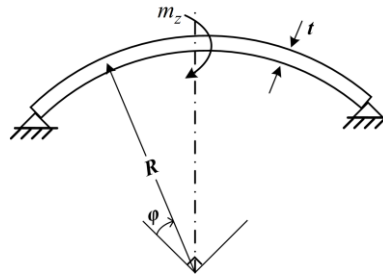


Fig. 5 The geometry of a simply supported quadrant beam subjected to the central concentrated moment

Table 1 Normalized displacements of a simply supported quadrant beam under load point

Type of Element	$u/u_c$	$\theta/\theta_c$
First Element	0.9997	1.0000
Second Element	0.9996	0.9991

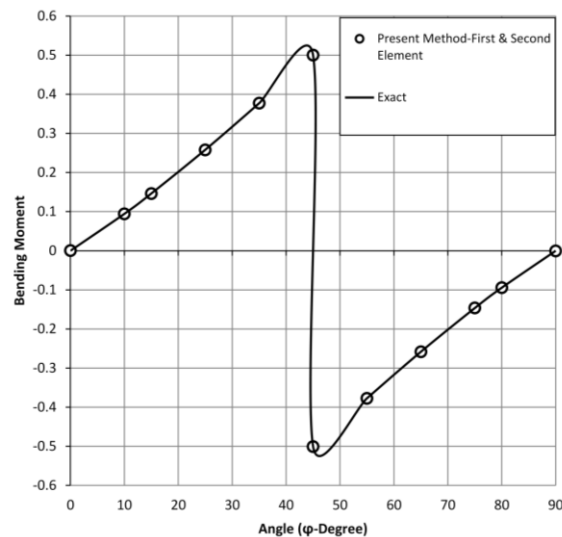


Fig. 6 Bending moment distribution of a simply supported quadrant beam over the arch length

Fig. 4, the error of the second element  $u/u_f$  is less than all the other similar results. Furthermore, based on the results, the superiority of second element for small  $R/t$  ratios is more evident in tangential displacement than radial displacement.

### 7.2 A moment discontinuity

Fig. 5 illustrates a simply supported quadrant beam with  $R=10$  and  $R/t=10000$ . Unit moment is applied to the structure's midpoint. To avoid the complexities of analyzing the indeterminate structure, the shear and axial effects are neglected in these equations. For the thin beam, the responses of the first and second author's elements can be normalized, as the same previous way. These are given in Table 1. The mechanical properties of this beam are considered as  $E=1.2E+10$

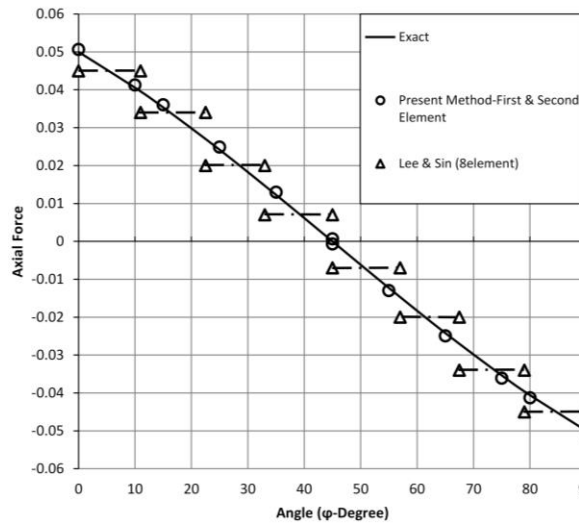


Fig. 7 Axial force distribution of a simply supported quadrant beam over the arch length

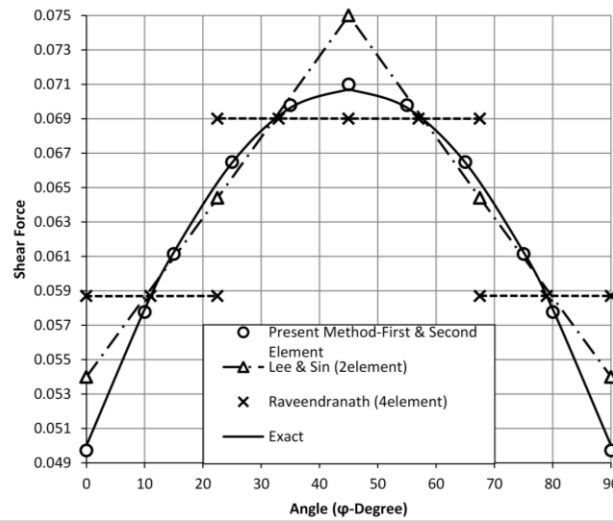


Fig. 8 Shear force distribution of a simply supported quadrant beam over the arch length

and  $G=4.615E+09$ . By employing two  $45^\circ$  elements, the internal forces over the structural arch length will be verified which is shown in Figs. 6-8. It should be added that the exact internal forces based on the energy's principles are obtained in the research of Lee and Sin research (1994).

### 7.3 A pinched ring

The geometry of a pinched ring, with unit width and  $R=0.127$  m (5in), is displayed in Fig. 9. This structure is subjected to a couple of compressive forces  $2q_y$ . This structure can be modeled by a quadrant circular arch with one nodal load  $q_y=45.36$  Kg (100lb), as it is seen in Fig. 9. By utilizing one element, the radial displacements of both ends will be calculated for a wide range of

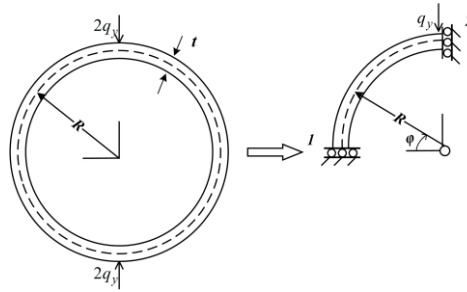


Fig. 9 The geometry of a pinched ring under a couple of compressive forces  $2q_y$

Table 2 The normalized radial displacements of the pinched ring by the first element, for a wide range of the slenderness ratio

Slenderness ratio ( $R/t$ )	Present method(one element used)		Lee and Sin (1994) (two element used)	
	$v_2/v_{c2}$	$v_1/v_{c1}$	$v_2/v_{c2}$	$v_1/v_{c1}$
2.5	0.99999	0.99999	0.99704	0.99740
5	1.00000	1.00000	0.99912	0.99932
10	1.00000	1.00000	0.99975	0.99983
20	1.00000	1.00000	0.99993	0.99995
100	1.00000	1.00000	1.00000	1.00000

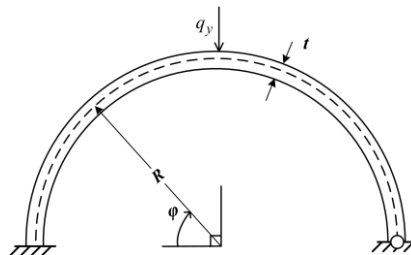


Fig. 10 The geometry of a semicircular beam under a central radial unit load

the slenderness ratio. In Table 2, the normalized answers of the first suggested element are compared against the results of Lee and Sin (1994), when they applied two elements. Mechanical properties of this pinched ring and the first benchmark problem are the same. It should be added that the answers are compared with the Castigliano's theorem that was used by Lee and Sin, as well (1994).

#### 7.4 A semicircular ring

To verify the efficiency of the author's formulations, the last test of the static case is a half-circle thin beam with a central unit load acting at the radial direction. The structural geometrical and mechanical characteristics are equal to the benchmark of section 7.2. As it is shown in Fig. 10, this semicircular ring does not have the symmetrical properties. To avoid the complexities of the Castigliano's theorem processes, only the bending effect is considered.

Fig. 11 indicates the results of the semicircular ring. The internal forces are verified, and the

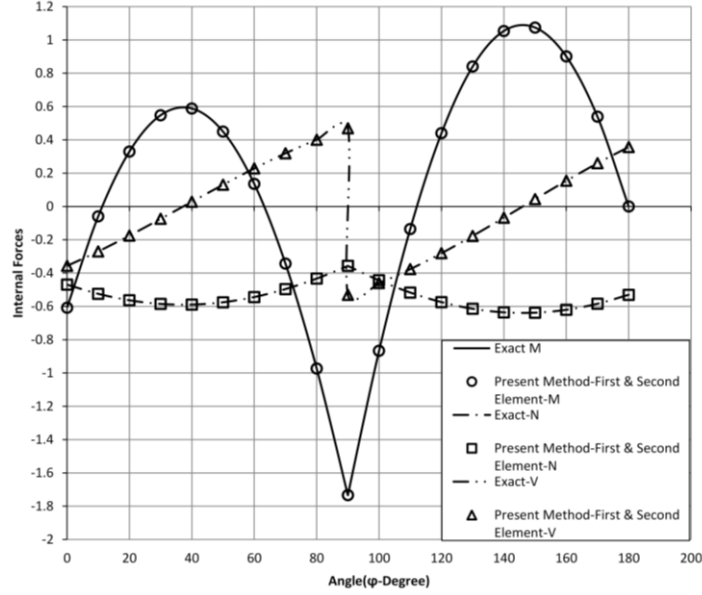


Fig. 11 Bending moment, axial and shear force distribution for the semicircular beam

exact values are given by the following relationships

$$X_1 = 0.5R \left( 1 - \frac{\pi^2}{4} + \frac{\pi}{2} \right) / \left( \frac{3\pi^2}{16} - 1 \right), X_2 = .5 \left( \frac{\pi}{2} - 1 \right) + X_1 \left( \frac{3\pi}{8R} \right) \quad (23)$$

$$M_z = \begin{cases} -0.5X_1(1 + \cos\varphi) + X_2(R \cdot \sin\varphi) + 0.5R(\cos\varphi - 1), & 0 \leq \varphi \leq \frac{\pi}{2} \\ -0.5X_1(1 - \sin\varphi) + X_2(R \cdot \cos\varphi) + 0.5R(\sin\varphi + 1), & \frac{\pi}{2} \leq \varphi \leq \pi \end{cases} \quad (24)$$

$$N_x = \begin{cases} -X_2(\sin\varphi) - 0.5 \left( 1 - \frac{X_1}{R} \right) \cos\varphi, & 0 \leq \varphi \leq \frac{\pi}{2} \\ -X_2(\cos\varphi) - 0.5 \left( 1 + \frac{X_1}{R} \right) \sin\varphi, & \frac{\pi}{2} \leq \varphi \leq \pi \end{cases} \quad (25)$$

$$V_y = \begin{cases} -X_2(\cos\varphi) + 0.5 \left( 1 - \frac{X_1}{R} \right) \sin\varphi, & 0 \leq \varphi \leq \frac{\pi}{2} \\ X_2(\sin\varphi) - 0.5 \left( 1 + \frac{X_1}{R} \right) \cos\varphi, & \frac{\pi}{2} \leq \varphi \leq \pi \end{cases} \quad (26)$$

The first four numerical tests were only statically analyzed. Based on these examples, it can be concluded that the first element is more efficient and usable due to almost exact answers and simple stiffness matrix. According to this outcome, dynamic analysis will be conducted by using first element.

Table 3 The first five non-dimensional natural frequencies for hinged-hinged and clamped-clamped supports

Boundary condition	Mode number $i$	Present method (20 element)	Yang <i>et al.</i> (2008) (10 4-nodded elements)	Eisenberger and Efraim (2001)
Hinged-Hinged	1	29.285	29.306	29.28
	2	33.321	33.243	33.305
	3	67.202	67.123	67.124
	4	80.049	79.95	79.971
	5	108.169	107.844	107.851
Clamped-Clamped	1	36.716	36.657	36.703
	2	42.278	42.289	42.264
	3	82.361	82.228	82.233
	4	84.565	84.471	84.491
	5	122.722	122.298	122.305

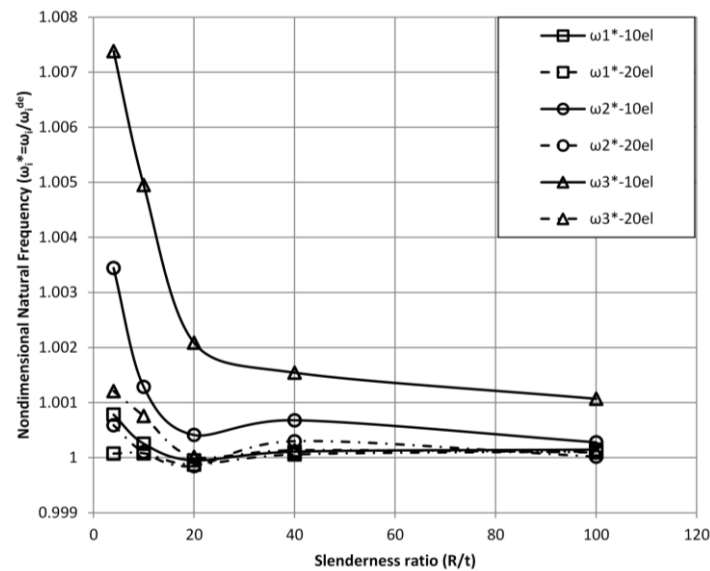


Fig. 12 Non-dimensional first three natural frequencies for hinged-hinged circular beam

### 7.5 The first free vibration test

In this part, two quarters of a circular beam with hinged-hinged and clamped-clamped boundary conditions are analyzed. It should be noted that the mechanical characteristics of  $E=70$  Gpa,  $k=0.85$ ,  $\nu=0.41666$  and  $\rho=2777$  kg/m<sup>3</sup> are equal for both boundary conditions. On the other hand,  $R=0.75$  m,  $A=4$  m<sup>2</sup> and  $I=0.01$  m<sup>4</sup> ( $R/t=4$ ), are for the hinged-hinged arch and  $R=0.6366$  m,  $A=1$  m<sup>2</sup> and  $I=0.0016$  m<sup>4</sup> ( $R/t=6$ ), are assumed for the clamped-clamped beam. To find the first five non-dimensional natural frequencies ( $\lambda_i=\omega_i t^2 \sqrt{\rho A/EI}$ ), a mesh with 20 elements is utilized. In Table 3, the author's answers are compared with the responses achieved by Yang *et al.* (2008), and also Eisenberger and Efraim (2001). Since the current study uses fewer degrees of freedom than before, the obtained frequencies are computed faster than mentioned solutions.

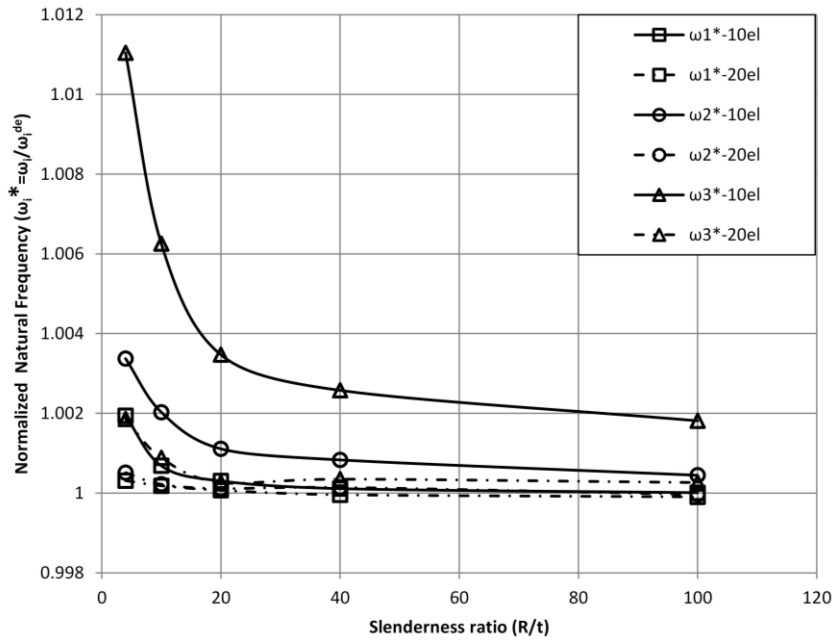


Fig. 13 Non-dimensional first three natural frequencies for clamped-clamped circular beam

### 7.6 The second free vibration test

In this example, the effect of  $R/t$  ratio on the answers of the curved members is studied. This ratio will change in the case of constant  $R$  and variable  $t$ . A square cross section with  $k=5/6$ ,  $\nu=0.3$ ,  $R=1$ ,  $E=1$  and  $\rho=1$  is used in this part. The variation of the first three natural frequencies ( $\omega_i^* = \omega_i / \omega_i^{de}$ ) of the calmped-clamped and hinged-hinged beams with  $\alpha=120^\circ$  versus the slenderness ratio ( $R/t$ ) are depicted in Figs. 12-13. According to the findings, by utilizing 10 and 20 elements, the results have higher precision in comparison with the Litewka & Rakowski (2001) answers, when 32 elements are used. It should be noted, the effects of shear and axial forces were considered in calculating  $\omega_i^{de}$ .

### 7.7 The third free vibration test

To demonstrate the suggested element's ability in solving thin and thick structures, a simply supported circular beam, with fixed  $R$  and  $A$ , is utilized. In this problem, the subtended angle is changing in the range of  $10^\circ$  to  $300^\circ$ , and the ratio of  $l/t$  will be variable, consequently. It should be noted, this ratio is minimum when  $\alpha=10^\circ$ , when the arch is considered as a thick curved beam. To clarify the superiority of presented method, the obtained results, when using three and six elements (12 and 21 D.O.F., respectively) are summarized in Table 4. Based on the findings, the fundamental frequency of the suggested element is in more agreement with THICK-2 (Leung and Zhu 2004) than EMC3c (Kim and Park 2008) and DCSQ2 (Kim and Lee 2008). The analysis are performed for  $R/t=48$ ,  $R=0.3048$  m,  $A=1.008E-04$  m<sup>2</sup>,  $I=4.162E-07$  m<sup>4</sup>,  $E=206.8$  GPa,  $\nu=0.3$ ,  $k=0.8497$  and  $\rho=0.2923$  Kg/m<sup>3</sup>. Also, to investigate the effect of curvature and boundary conditions on the natural frequency, the ratio  $l/t$  is considered equal to 84. It should be mentioned,

Table 4 Fundamental frequency (rad/s) of a simply supported circular beam

Subtended Angle (degrees)	Present Method (12 d.o.f.)	Present Method (21 d.o.f.)	Kim and Lee (2008) (DCSQ2-12d.o.f)	Kim and Park (2008) (EMC3c-21 d.o.f)	Leung and Zhu (2004) (THICK-2)
10	5857.8064	5844.6136	-----	5842.0000	5841.7400
20	2842.3698	2829.4683	-----	2826.5000	2827.6300
30	2369.5550	2342.6348	2370.0100	2342.8000	2339.8200
60	563.7779	560.5859	564.0500	561.9200	560.2500
90	230.1236	229.7332	230.3100	230.7500	229.6600
120	115.7120	115.6542	115.8200	116.1800	115.6400
180	37.8607	37.8558	37.9100	38.0200	37.8600
240	13.6621	13.6613	13.6900	13.7200	13.6600
270	7.9219	7.9216	7.0400	7.9500	7.9200
300	4.1847	4.1846	4.2000	4.2000	4.1800

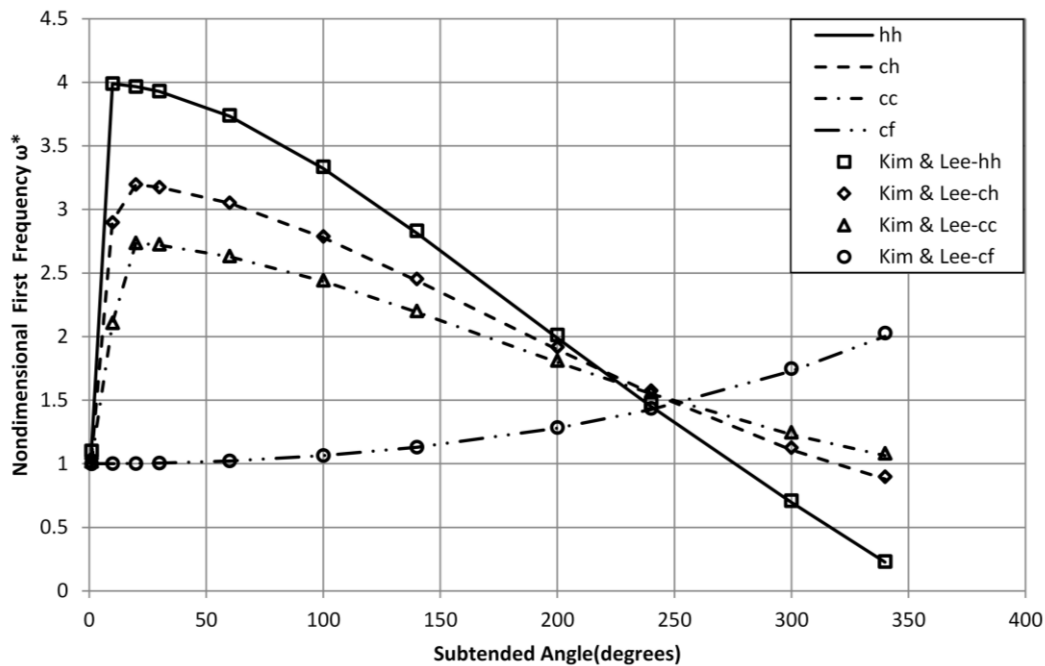


Fig. 14 The effect of curvature and boundary condition on the first natural frequencies of a circular beam

the member's length and area of the cross section always remain unchanged. Therefore, the variations of the subtended angle and  $R$  determine the curvature of the beam. As it is shown in Fig. 14, by utilizing six elements, the obtained answers are in good agreement with Kim and Lee (2008) for the identical discretization. The vertical axis shows  $\omega^*$ , which is the ratio of fundamental frequency of the curved beam to the straight beam with the same length and boundary conditions.

## 8. Conclusions

Two novel element formulations for the circular beam, with two nodes, six degrees of freedom and rectangular cross section were developed. Due to utilizing equilibrium conditions and dependency of the displacement's functions, no locking error or excessive stiffening effects could enter the answers. The presented methods were verified by solving four static problems. Results of the first recommended element were compared with the exact solutions. To validate more the offered procedure, the answers of second presented element were verified by comparing them with the outcomes of the finite element scheme, when a fine mesh is used.

According to the numerical results, the internal forces of both suggested elements were superior in comparison to the other available solutions. This valuable act is rooted on the incorporating equilibrium condition in developing the author's elements. It should be added that in the thick structure, the performance of the second recommended element was desirable. In contrast, the response of the first one, particularly for the tangential displacement, was unsuitable. However, the results of both proposed elements were similar for the thin structures. Findings clearly demonstrate that the first element can be used in a wide range of the slenderness ratio for the circular beams except for too thick ones. Another merit of the author's approach is that employing only one of these two elements is adequate to achieve the precise answers for any circular beams. It is obvious that the obtained closed-form structural stiffness matrix is a strong tool for solving circular beams with complicated boundary conditions in a minimum time. The first element's stiffness matrix is simpler and shorter than the second one. So, it is given in Appendix 1 to facilitate the future analysis. Based on static responses, it was clearly deduced that the first element is efficient and usable for all the range of different structural characteristics. Therefore, the free vibration analysis was performed by using the first presented element. Some tests are given to investigate the effect of some specifications on the natural frequencies of the circular beam, such as, boundary conditions, curvature and slenderness ratio. The results are in more agreement with the exact values than the previously published ones. All the results of static and dynamic tests show no deficiency, such as, shear and membrane locking and excessive stiff structural behavior.

## References

- Ashwell, D.G. and Sabir, A.B. (1971), "Limitations of certain curved finite elements when applied to arches", *Int. J. Mech. Sci.*, **13**, 133-139.
- Benedetti, A. and Tralli, A. (1989), "A new hybrid F.E. model for arbitrarily curved beam-i. linear analysis", *Comput. Struct.*, **33**(6), 1437-1449.
- Choi, J.K. and Lim, J.K. (1993), "Simple curved shear beam elements", *Commun. Numer. Meth. Eng.*, **9**, 659-669.
- Choi, J.K. and Lim, J.K. (1995), "General curved beam elements based on the assumed strain fields", *Comput. Struct.*, **55**(3), 379-386.
- Dawe, D.J. (1974), "Curved finite elements for the analysis of shallow and deep arches", *Comput. Struct.*, **4**, 559-580.
- Eisenberger, M. and Efraim, E. (2001), "In-plane vibrations of shear deformable curved beams", *Int. J. Numer. Meth. Eng.*, **52**, 1221-1234.
- Gimena, L., Gonzaga, P. and N. Gimena, F. (2010), "Forces, moments, rotations, and displacements of polynomial-shaped curved beams", *Int. J. Struct. Stab. Dyn.*, **10**(1), 77-89.
- Gonzaga, P., Gimena, F.N. and Gimena, L. (2014), "Stiffness and transfer matrix analysis in global

- coordinates of a 3D curved beam”, *J. Struct. Stab. Dyn.*, **14**(7), 1450019.
- Heppler, G.R. (1992), “An element for studying the vibration of unrestrained curved Timoshenko beams”, *J. Sound Vib.*, **158**(3), 387-404.
- Ishaquddin, M., Raveendranath, P. and Reddy, J.N. (2013), “Coupled polynomial field approach for elimination of flexure and torsion locking phenomena in the Timoshenko and Euler-Bernoulli curved beam elements”, *Finite Elem. Anal. Des.*, **65**, 17-31.
- Jafari, M. and Mahjoob, M.J. (2010), “An exact three-dimensional beam element with nonuniform cross section”, *J. Appl. Mech.*, **77**(6), 061009.
- Kim, J.G. and Kim, Y.Y. (1998), “A new higher-order hybrid-mixed curved beam element”, *Int. J. Numer. Meth. Eng.*, **43**, 925-940.
- Kim, J.G. and Lee, J.K. (2008), “Free-vibration analysis of arches based on the hybrid-mixed formulation with consistent quadratic stress functions”, *Comput. Struct.*, **86**, 1672-1681.
- Kim, J.G. and Park, Y.K. (2008), “The effect of additional equilibrium stress functions on the three-node hybrid-mixed curved beam element”, *J. Mech. Sci. Tech.*, **22**, 2030-2037.
- Kim, J.G., Lee, J.K. and Yoon, H.J. (2014), “On the effect of shear coefficients in free vibration analysis of curved beams”, *J. Mech. Sci. Tech.*, **28**(8), 3181-3187.
- Krishnan, A. and Suresh, Y.J. (1998), “A simple cubic linear element for static and free vibration analyses of curved beams”, *Comput. Struct.*, **68**, 473-489.
- Lee, P.G. and Sin, H.C. (1994), “Locking-free curved beam element based on curvature”, *Int. J. Numer. Meth. Eng.*, **37**, 989-1007.
- Leung, A.Y.T. and Zhu, B. (2004), “Fourier p-elements for curved beam vibrations”, *Thin Wall. Struct.*, **42**, 39-57.
- Litewka, P. and Rakowski, J. (1998), “The exact thick arch finite element”, *Comput. Struct.*, **68**, 369-379.
- Litewka, P. and Rakowski, J. (2001), “Free vibrations of shear-flexible and compressible arches by FEM”, *Int. J. Numer. Meth. Eng.*, **52**, 273-286.
- Meck, H.R. (1980), “An accurate polynomial displacement function for finite ring elements”, *Comput. Struct.*, **11**, 265-269.
- Pandian, N., Appa Rao, T.V.S.R. and Chandra, S. (1989), “Studies on performance of curved beam finite elements for analysis of thin arches”, *Comput. Struct.*, **31**(6), 997-1002.
- Raveendranath, P., Singh, G. and Pradhan, B. (1999), “A two-noded locking-free shear flexible curved beam element”, *Int. J. Numer. Meth. Eng.*, **44**, 265-280.
- Raveendranath, P., Singh, G. and Rao, G.V. (2001), “A three-noded shear flexible curved beam element based on coupled displacement field interpolations”, *Int. J. Numer. Meth. Eng.*, **51**, 85-101.
- Reddy, J.N. (1993), *An Introduction to the Finite Element Method*, McGraw-Hill, Inc.
- Sabir, A.B. and Ashwell, D.G. (1971), “A comparison of curved beam finite elements when used in vibration problems”, *J. Sound Vib.*, **18**(4), 555-563.
- Stolarski, H. and Belytschko, T. (1982), “Membrane locking and reduced integration for curved beams”, *J. Appl. Mech.*, **49**, 172-176.
- Yang, F., Sedaghati, R. and Esmailzadeh, E. (2008), “Free in-plane vibration of general curved beams using finite element method”, *J. Sound Vib.*, **318**, 850-867.
- Yang, S.Y. and Sin, H.C. (1995), “Curvature-based beam elements for the analysis of Timoshenko and shear-deformable curved beams”, *J. Sound Vib.*, **18**, 7569-84.
- Zhu, Z.H. and Meguid, S.A. (2008), “Vibration analysis of a new curved beam element”, *J. Sound Vib.*, **309**, 86-95.

**Appendix 1. Closed-form entries of the first element stiffness matrix**

$$G_{11} = \frac{1}{D_1} (2.(2.\beta R \cos^2(\alpha) + 2.\alpha\mu \sin(\alpha) \cos(\alpha) - 4.\beta R \cos(\alpha) - \lambda\alpha \sin(\alpha) \cos(\alpha) + 2.\beta R - \lambda\alpha^2 + 2.\alpha\beta R \sin(\alpha) \cos(\alpha)))$$

$$G_{12} = \frac{1}{D_1} (2.\sin(\alpha)(-2.\beta R + 2.\beta R \cos(\alpha) - \alpha\lambda \sin(\alpha) + 2.\beta R\alpha \sin(\alpha) + 2.\alpha\mu \sin(\alpha)))$$

$$G_{13} = \frac{-1}{D_1} (2.R(2.\mu \cos^2(\alpha) - \lambda \cos^2(\alpha) + 4.\beta R \cos^2(\alpha) - \lambda\alpha \sin(\alpha) \cos(\alpha) - 4.\beta R \cos(\alpha) + 2.\alpha\beta R \sin(\alpha) \cos(\alpha) + 2.\alpha\mu \sin(\alpha) \cos(\alpha) + \lambda - 2.\mu + \alpha\lambda \sin(\alpha) - \lambda\alpha^2))$$

$$G_{14} = \frac{-1}{D_1} (2.(-2.\beta R \cos^2(\alpha) + 4.\beta R \cos(\alpha) - \lambda\alpha^2 \cos(\alpha) - \alpha\lambda \sin(\alpha) - 2.\beta R + 2.\alpha\beta R \sin(\alpha) + 2.\alpha\mu \sin(\alpha)))$$

$$G_{15} = \frac{-1}{D_1} (2.\sin(\alpha)(2.\beta R \cos(\alpha) + \lambda\alpha^2 - 2.\beta R))$$

$$G_{16} = \frac{1}{D_1} (2.R(2.\mu \cos^2(\alpha) - \lambda \cos^2(\alpha) - \lambda\alpha^2 \cos(\alpha) + 4.\beta R \cos(\alpha) + \lambda - 4.\beta R - 2.\mu + 2.\alpha\beta R \sin(\alpha) + 2.\alpha\mu \sin(\alpha)))$$

$$G_{21} = -G_{12}$$

$$G_{22} = \frac{1}{D_1} (2.(2.\beta R \cos^2(\alpha) + 2.\alpha\mu \sin(\alpha) \cos(\alpha) - \lambda\alpha \sin(\alpha) \cos(\alpha) - 2.\beta R + 2.\alpha\beta R \sin(\alpha) \cos(\alpha) + \lambda\alpha^2))$$

$$G_{23} = \frac{1}{D_1} (2.R(2.\beta R\alpha - 2.\beta R\alpha \cos^2(\alpha) - 4.\beta R \sin(\alpha) + 4.\beta R \sin(\alpha) \cos(\alpha) + \alpha\lambda \cos^2(\alpha) - \lambda\alpha \cos(\alpha) + 2.\mu \sin(\alpha) \cos(\alpha) - \lambda \sin(\alpha) \cos(\alpha) - 2.\mu\alpha \cos^2(\alpha) + 2.\mu\alpha - 2.\mu \sin(\alpha) + \lambda \sin(\alpha)))$$

$$G_{24} = G_{15}$$

$$G_{25} = \frac{-1}{D_1} (2.(2.\beta R \cos^2(\alpha) + \lambda\alpha^2 \cos(\alpha) - \alpha\lambda \sin(\alpha) - 2.\beta R + 2.\alpha\beta R \sin(\alpha) + 2.\alpha\mu \sin(\alpha)))$$

$$G_{26} = \frac{-1}{D_1} (2.R(-2.\mu \sin(\alpha) + 2.\mu \sin(\alpha) \cos(\alpha) + \lambda \sin(\alpha) - \lambda\alpha^2 \sin(\alpha) - \lambda \sin(\alpha) \cos(\alpha) - \lambda\alpha \cos(\alpha) + \lambda\alpha))$$

$$G_{31} = \frac{-1}{D_2} (2.R \sin(\alpha)), G_{32} = \frac{1}{D_2} (2.R(-1 + \cos(\alpha))), G_{33} = \frac{-R}{\beta D_2} (2.\mu \sin(\alpha) - \lambda \sin(\alpha) + \lambda\alpha)$$

$$G_{34} = -G_{31}, G_{35} = G_{32}, G_{36} = -G_{33}$$

$$D_1 = \alpha \cos^2(\alpha)(-4\beta^2 R^2 + \beta R(4.\lambda - 8.\mu) + 4.\mu\lambda - 4\mu^2 - \lambda^2) + \cos(\alpha)(\sin(\alpha)(8.\beta^2 R^2 + \beta R(8.\mu - 4.\lambda)) - 4.\beta R\lambda\alpha) + \sin(\alpha)(-8.\beta^2 R^2 + \beta R(4.\lambda - 8.\mu) - \lambda^2\alpha^3 + \alpha(4.\beta^2 R^2 + 8.\beta R\mu + 4.\mu^2 - 4.\mu\lambda + \lambda^2))$$

$$D_2 = 4.\beta R \cos(\alpha) - \lambda \alpha \sin(\alpha) + 2.\beta R \alpha \sin(\alpha) + 2\alpha \mu \sin(\alpha) - 4.\beta R + \lambda \alpha^2$$

$$S_{ij} = I_1 \left( \frac{G_{2i} G_{2j} R}{EA} + \frac{G_{1i} G_{1j} R}{kGA} + \frac{G_{2i} G_{2j} R^3}{EI} \right) + I_2 \left( \frac{G_{1i} G_{1j} R}{EA} + \frac{G_{2i} G_{2j} R}{kGA} + \frac{G_{1i} G_{1j} R^3}{EI} \right)$$

$$+ I_3 \left( -\frac{R}{EA} + \frac{R}{kGA} - \frac{R^3}{EI} \right) (G_{1i} G_{2j} + G_{2i} G_{1j}) - \frac{I_4 R^2 (G_{2i} G_{3j} + G_{3i} G_{2j})}{EI} + \frac{I_5 R^2 (G_{1i} G_{3j} + G_{3i} G_{1j})}{EI}$$

$$+ \frac{\alpha R (G_{3i} G_{3j})}{EI}, i, j = 1, 2, 3$$

$$I_1 = 0.25(2.\alpha - \sin(2\alpha)), I_2 = 0.25(2.\alpha + \sin(2\alpha)), I_3 = 0.25(1 - \cos(2\alpha)), I_4 = 1 - \cos(\alpha), I_5 = \sin(\alpha)$$